# Theory of Optical Trapping by an Optical Vortex Beam

Jack Ng,[1] Zhifang Lin,[1,2,3] and C. T. Chan[1]

[1]*Department of Physics and William Mong Institute of Nano Science & Technology, Hong Kong University of Science and Technology,
Clear Water Bay, Hong Kong, China*
[2]*Department of Physics, Fudan University, Shanghai, China*
[3]*Key Laboratory of Micro and Nano Photonic Structures (Ministry of Education), Fudan University, Shanghai, China.*
(Received 10 September 2009; published 10 March 2010)

We propose a theory to explain optical trapping by optical vortices (OVs), which are emerging as important tools to trap mesoscopic particles. The common perception is that the trapping is solely due to the gradient force and that it may be characterized by three real force constants. However, we show that the OV trap can exhibit complex force constants, implying that the trapping must be stabilized by ambient damping. At different damping levels, particles exhibit remarkably different dynamics, such as stable trapping and periodic and aperiodic orbital motions.

Optical tweezers are a powerful tool for trapping mesoscopic objects [1]. Applications of optical tweezers range from the trapping and cooling of atoms to capturing large molecules such as DNA and microscopic particles and biological objects [2–4]. As new methods to create beam profiles are being introduced, more exotic beams are used to trap particles and many of them, known as optical vortices (OVs), have angular momentum (AM) [5–14]. We show that although the conventional stiffness constant approach works for a Gaussian beam [15,16], the theory of trapping by an OV is more complex. In the conventional approach, optical traps are usually characterized by three stiffness constants along the three principal axes. Although this approach is quite accurate in describing ordinary optical tweezers, we shall see that for an OV, the principal axes are not even "real". The theoretical procedure to obtain the principal axes is to diagonalize the force constant matrix, $K_{ij} = \partial f_{\text{light},i}/\partial x_j$, at equilibrium, where $f_{\text{light},i}$ and $x_i$ are, respectively, the $i$th Cartesian component of the optical force and the particle displacement away from the equilibrium position. The eigenvalues of the force constant matrix give the eigen force constants (EFCs, or trap stiffness), while the eigenmodes determine the principal axes. We use force constant matrix formalism to study OV trapping [17–23] and find that the difference between the conventional approach and our treatment is a qualitative one, to the extent that the EFCs can be complex numbers and we have to abandon concepts such as the parabolic potential for the transverse directions. By analyzing the stability and by simulating the dynamics of a particle trapped by OVs, it is found that the trapping stability of OVs generally depends on the ambient damping. In particular, in the presence of AM, the optical trapping may exhibit a fascinating variety of phenomena ranging from "opto-hydrodynamic" trapping (where the trapping is stabilized by the ambient damping) to supercritical Andronov-Hopf bifurcation (where a periodic orbit is created as ambient damping decreases) [24].

To illustrate the basic idea, let us start from the linear stability analysis. Consider a trapped particle, near an equilibrium trapping (zero-force) position. The optical and damping forces are $\vec{F} = md^2\Delta\vec{x}/dt^2 \approx \overleftrightarrow{K}\Delta\vec{x} - \gamma d\Delta\vec{x}/dt$, where $m$ is the mass of the particle, $\Delta\vec{x}$ is the particle's displacement from the equilibrium, $\overleftrightarrow{K}\Delta\vec{x}$ is the optical force, and $\gamma$ is the ambient damping constant. Here we neglect the thermal fluctuation, as it is small compared to the optical force for an intense laser. The eigenvalues, $K_i$, of the force matrix, $\overleftrightarrow{K}$, are precisely the EFCs and the eigenvectors of $\overleftrightarrow{K}$ are the eigenmodes. For a trapping beam propagating along $\hat{z}$, the force constant matrix has the general form

$$\overleftrightarrow{K} = \begin{bmatrix} a & d & 0 \\ g & b & 0 \\ e & f & c \end{bmatrix}, \tag{1}$$

where all elements are real numbers. The elements $\partial f_{\text{light},x}/\partial z$ and $\partial f_{\text{light},y}/\partial z$ are zeros by symmetry, because there is no induced force along the transverse plane as the particle is displaced along $\hat{z}$. The elements $e$ and $f$ are also zero by symmetry in Laguerre Gaussian (LG) and Gaussian beams, but as they do not enter into in the following discussion of the eigenvalues, we will not specify their values. The diagonal elements, $a$, $b$, and $c$, characterize three restoring forces, which are usually taken as the three stiffness constants in the conventional approach [25]. The off-diagonal elements, $d$ and $g$, characterize the rotational torques: as the particle is displaced along $x$ ($y$), it experiences a torque that manifests as a force along the $y$ ($x$) direction. As an OV carries orbital AM, the beam energy propagates spirally along the beam axis, resulting in a rotating energy flux in the transverse plane. This rotating energy flux exerts a torque on the particle, implying nonzero matrix components $d$ and $g$. On the other hand, $d = g = 0$ for beams that have no AM.

By diagonalizing Eq. (1), we obtain three EFCs: $K_{\text{axial}} = c$ and $K_{\text{trans}\pm} = [a + b \pm \sqrt{(a-b)^2 + 4dg}]/2$. Conservative mechanical systems can be described by the potential energy, $U$, and their force constant matrix is a real symmetric matrix (i.e., $K_{ij} = -\partial^2 U/\partial x_i \partial x_j = K_{ji}$). It then follows that all eigenvalues are real. However, the optical force is nonconservative as the particle can obtain energy from the beam, and its $\overset{\leftrightarrow}{K}$ is, in general, a real but nonsymmetric matrix. Consequently, its eigenvalues can have conjugate pairs of complex numbers. It can be seen that when

$$-4dg > (a-b)^2, \qquad (2)$$

$K_{\text{trans}\pm}$'s are a conjugate pair of complex numbers. Thus, in general, an optically trapped particle may not be characterized by three real force constants if the beam has AM. For beams that have no AM, $d = g = 0$, all the EFCs are real numbers. On the other hand, an OV beam, well known for its AM characteristic, leads to nonzero $d$ and $g$, and thus (2) can be fulfilled under certain conditions. The existence of complex EFCs implies that the common notion of a parabolic potential in an optical trap is no longer meaningful. Whether or not complex EFCs occur depends on the competition between the beam asymmetry and the AM. Equation (2) cannot be fulfilled when $|a - b|$ is large. Since $a$ and $b$ are the restoring force constants for the $x$ and $y$ directions, respectively, a large $|a - b|$ implies a large asymmetry between the two coordinate axes. The underlining physics is that, with large asymmetry, the beam can pin a particle to one of its axes, preventing it from "falling" into the OV. On the contrary, if there is weak or no asymmetry ($|a - b| \simeq 0$), the trapped particle is not tied to the coordinate axis, and will thus be pushed to rotate by the OV. As a result, its AM and energy will accumulate. If there is no dissipation ($\gamma = 0$), the particle will orbit around the beam center with increasing speed and eventually escape from the trap [26]. We therefore conclude that, in general, the OV trapping cannot be achieved solely by light. It is the dissipation in the suspending medium that keeps the particle's kinetic energy and AM bounded, rendering the particle trapped [26]. Such a state of OV trapping is believed to be what the experiments observed, instead of pure gradient force trapping. For the case of circularly polarized beams (LG or Gaussian), cylindrical symmetry mandates that $|a - b| = 0$, implying that the transverse EFCs are always complex. This means that circularly polarized beams cannot trap a particle without the dissipation of the medium in which the particle is dispersed. More mathematical details can be found in our online materials [27].

We now proceed to show, using heavy numerical simulations, concrete examples in which the EFCs are indeed complex. We model the incident trapping beam by using the highly accurate generalized vector Debye integral [28,29], where the focusing of the incident laser beam by the high numerical aperture (NA) object lens is treated

using geometrical optics, and then the focused field near the focal region is obtained using the angular spectrum representations. The use of geometrical optics in beam focusing is fully justified as the lens is macroscopic in size, and all remaining parts of our theory employ classical electromagnetic optics. With the strongly focused beam given by the vector Debye integral, Mie theory is then used to calculate the scattered field, and then Maxwell stress tensor formalism is used to compute the optical force [30,31]. We note that the formalisms we use have been proven to agree well with experiments [15,16,29,32]. Figure 1(a) shows $K_{\text{trans}\pm}$ for an LG beam focused by a high NA water immersion objective. The beam is linearly polarized with wavelength $\lambda = 1064$ nm, topological charge $l = 1$, NA $= 1.2$, and filling factor $f = 1$. The trapping is in water ($\varepsilon_{\text{water}} = 1.33^2$) and the sphere is made of polystyrene ($\varepsilon_{\text{sphere}} = 1.57^2$ and mass density $\rho = 1050$ kg m$^{-3}$). The axial EFC is not plotted, as it is always real and negative, indicating that the particle can be trapped along the axial direction solely by gradient forces. It can be clearly seen from Fig. 1(a) that at certain ranges of particle sizes, $\text{Im}\{K_{\text{trans}\pm}\} \neq 0$, and this numerical result reflects the assertion that the OV trap cannot be characterized by three real force constants in general. At these particle sizes, $K_{\text{trans}+} = K_{\text{trans}-}^*$, and the two curves corresponding to $\text{Re}\{K_{\text{trans}\pm}\}$ merge together. We note that only the absolute value of $\text{Im}\{K_{\text{trans}\pm}\}$ is plotted in Fig. 1(a). When the EFCs are all real numbers, the behavior of the trapped particle is qualitatively similar to that of the ordinary optical trapping by conventional optical tweezers. This corresponds to the scenario that either the beam's AM is weak (small $d$ and $g$), or the asymmetry of the beam ($|a - b|$) is large. We note that the existence of the region where $\text{Im}\{K_{\text{trans}\pm}\} \neq 0$ implies that in low viscosity media, only particles of certain sizes can be trapped. For complex EFCs, the eigenmodes corresponding to the complex EFCs are [27]

$$\Delta \overrightarrow{x}_\pm(t) = A_\pm e^{-\text{Im}(\Omega_\pm)t}\{\text{Re}(\overrightarrow{V})\sin[\text{Re}(\Omega_\pm)t + \phi_\pm]$$

$$+ \text{Im}(\overrightarrow{V})\cos[\text{Re}(\Omega_\pm)t + \phi_\pm]\}, \qquad (3)$$
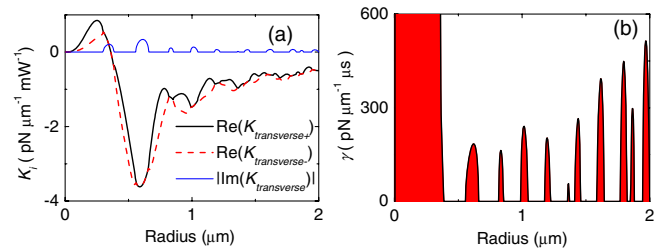


FIG. 1 (color online). The incident beam is a linearly polarized LG beam with $\lambda = 1064$ nm, $l = 1$, $f = 1$, and NA $= 1.2$. (a) The transverse EFCs. (b) Phase diagram for a particle trapped at a power of 1 W. The white (red) regions are stable (unstable). The black line marks $\gamma_{\text{critical}}$.

where $\overset{\rightarrow}{V}$ is the eigenvector corresponding to eigenvalue $K_i$ of the force constant matrix, $\overset{\leftrightarrow}{K}$. $\{A_{\pm}, \phi_{\pm}\}$ are determined from the initial conditions, and

$$\mathrm{Re}(\Omega_{\pm}) = \mp(\Delta_R{}^2 + \Delta_I{}^2)^{1/4}\sin(\delta/2)/2m,$$
$$\mathrm{Im}(\Omega_{\pm}) = \gamma \pm (\Delta_R{}^2 + \Delta_I{}^2)^{1/4}\cos(\delta/2)/2m, \quad (4)$$

$$\delta = \begin{cases} \tan^{-1}(\Delta_I/\Delta_R), & \text{if } \Delta_R > 0, \\ \pi - \tan^{-1}(\Delta_I/|\Delta_R|), & \text{if } \Delta_R < 0, \end{cases} \quad (5)$$

where $\Delta_I = 4m\mathrm{Im}\{K_i\}$ and $\Delta_R = \gamma^2 + 4m\mathrm{Re}\{K_i\}$. The modes are stable if and only if both $\mathrm{Im}(\Omega_{\pm}) > 0$. If $\mathrm{Re}\{K_i\} > 0$, one of the two modes is always unstable such that, upon small perturbation, the particle will spiral outward and leave the trap. If $\mathrm{Re}\{K_i\} < 0$, the mode is unstable for $\gamma < \gamma_{\mathrm{critical}} = \sqrt{m}|\mathrm{Im}\{K_i\}|/\sqrt{|\mathrm{Re}\{K_i\}|}$. However, this equilibrium can be stabilized by increasing $\gamma$ to beyond $\gamma_{\mathrm{critical}}$. We label this kind of mode as a quasistable mode, in which the stability of the mode depends on the ambient damping. The complex modes described by Eq. (3) correspond to spiral motions, which means that the particle acquires AM from the beam. The converse is also true: these spiral modes can exist only when the particle can acquire AM. We note that the particle can acquire AM from the beam because the Poynting vector of an OV propagates spirally along the beam axis, resulting in a rotating energy flux in the transverse plane. This rotating energy flux exerts a torque on the particle, implying the transfer of angular momentum from the beam to the particle.

We note in Fig. 1 that in our specific example, $\mathrm{Re}\{K_{\mathrm{trans}\pm}\} > 0$, for sphere radius $R < 0.36$ $\mu$m [the radius of the intensity ring $\sim 0.33$ $\mu$m, see Fig. 2(a)], which means that small dielectric particles are unstable, as reported by experiments [14]. We note that in previous experiments on the trapping of a strongly absorptive particle, the particle is unstable along the axial direction. Accordingly, other forces, such as a repulsive force from a substrate, are needed to stabilize the particle. However, in this Letter, we consider transverse optical trapping. Our conclusion is thus valid irrespective of the nature of the axial trapping. The small dielectric particles are attracted by the high intensity ring and, under sufficient damping, these small particles will orbit along the ring [14]. On the other hand, $\mathrm{Re}\{K_i\} < 0$ for $R > 0.36$ $\mu$m. The sphere is bigger than the intensity ring, so that the gradient force drives the sphere to the beam center. A phase diagram for the optically trapped particle is given in Fig. 1(b). At $R = 0.36$ $\mu$m, $\gamma_{\mathrm{critical}} \to \infty$ as $\mathrm{Re}\{K_{\mathrm{trans}\pm}\} \to 0$. The equilibrium point at $(x, y) = (0, 0)$ is unstable for $R < 0.36$ $\mu$m at any value of damping. For $R > 0.36$ $\mu$m, the white (shaded) region where $\gamma > \gamma_{\mathrm{critical}}$ ($\gamma < \gamma_{\mathrm{critical}}$) is the regime where the damping is sufficient (insufficient) to stabilize the particle. We note that when the EFC is real, no damping is required for stability since $\gamma_{\mathrm{critical}} = 0$. According to Stoke's law, the damping constant of water
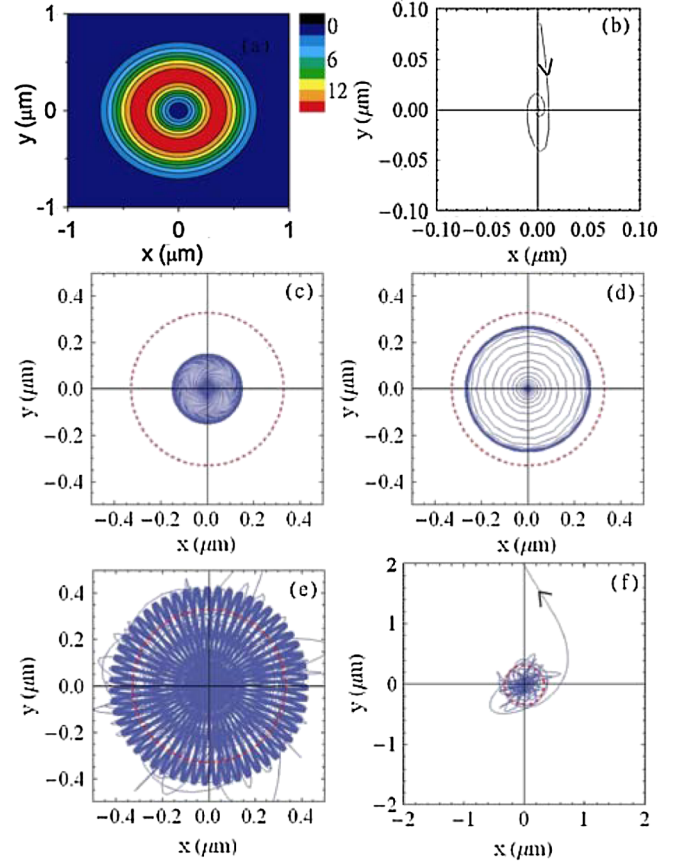


FIG. 2 (color online). (a) The focal plane intensity (arbitrary units) of a right polarized LG beam with $\lambda = 1064$ nm, $l = 1$, $f = 1$, and NA $= 1.2$. (b)–(f) The trajectory (blue [dark gray]) of a 1-micron-diameter particle trapped by a 550 mW beam. The red dotted lines show the approximate radius of the intensity ring of the trapping beam. The damping constants $\gamma$ for each panel, in units of pN $\mu$s/$\mu$m, are given by (b) 550, (c) 110, (d) 55, (e) 5.5, and (f) 0. The arrows in (b) and (f) indicate the direction of motion.

and air are, respectively, $1.9 \times 10^4 R$ (pN $\mu$s/$\mu$m$^2$) and $3.3 \times 10^2 R$ (pN $\mu$s/$\mu$m$^2$). The damping of water is much larger than $\gamma_{\mathrm{critical}}$ plotted in Fig. 1(b), and thus unless we use high laser power, we shall observe stable trapping in water, in agreement with existing experiments. The damping of air is of the same order of magnitude of $\gamma_{\mathrm{critical}}$ plotted in Fig. 1(b). Consequently, for an experiment conducted in air, we shall be able to see the transition between the stable and unstable state, depending on the laser power employed.

It is now clear that a particle trapped by an OV is stable if $\gamma > \gamma_{\mathrm{critical}}$ and unstable if $\gamma < \gamma_{\mathrm{critical}}$. Nevertheless, the case of $\gamma \approx \gamma_{\mathrm{critical}}$ is nonhyperbolic (the linear term vanishes), and thus the higher order terms are important. In that case, we numerically integrate the full equation of motion, $md^2\overset{\rightarrow}{\Delta x}/dt^2 = \overset{\rightarrow}{f}_{\mathrm{light}} - \gamma d\overset{\rightarrow}{\Delta x}/dt$, using an adaptive time step Runge-Kutta-Verner algorithm [30]. Figure 2(a) shows the field intensity on the focal plane for a right circularly polarized LG beam, with a dark central spot

and a high intensity ring of radius $\sim$0.33 $\mu$m. Figures 2(b)–2(f) show the trajectories of a 1-$\mu$m-diameter particle illuminated by the LG beam (power = 550 mW), in the order of decreasing damping. When there is strong damping, as shown in Fig. 2(b) where $\gamma = 550$ pN $\mu$s/$\mu$m, the trapped sphere exhibits damped oscillation upon small perturbation and settles into a stable equilibrium position. For weaker damping, the sphere initially spirals outward and then settles into a periodic circular orbit [see Fig. 2(c) where $\gamma = 110$ pN $\mu$s/$\mu$m]. Such bifurcation of a stable equilibrium into an unstable equilibrium and a stable periodic orbit is known as a supercritical Andronov-Hopf bifurcation [24,30]. If we further reduce the damping, the radius of the circular orbit increases, as shown in Fig. 2(d) where $\gamma = 55$ pN $\mu$s/$\mu$m. If the damping decreases further, the particle goes into an exotic orbit around the intensity ring, as shown in Fig. 2(e) where $\gamma = 5.5$ pN $\mu$s/$\mu$m. When there is no damping [see Fig. 2(f), $\gamma = 0$ pN $\mu$s/$\mu$m], the particle initially fluctuates around the equilibrium with increasing amplitude and eventually escapes from the trap due to the accumulation of AM. If a small imaginary part is added to the dielectric constant of the particle, the scattering and absorption force will be enhanced. As a result the particle is being pushed to move further away from the focus, where the angular momentum density is weaker, and this will result in a slower rate of angular momentum transfer. In other words, a small amount of absorption may in fact favor the transverse trapping, though it degrades the axial trapping. Finally, we note that with absorption, the particle will also spin along its own axis.

Our analysis reveals that the EFCs for a beam with AM can be complex numbers. In the case of complex EFCs, when there is sufficient (insufficient) damping, a particle can (cannot) be stably trapped. There is an intermediate range of damping in which the particle will be driven into exotic periodic or aperiodic orbital motions. Finally, we note that as the ambient damping force plays an important role in OV trapping, it should be more accurately termed "opto-hydrodynamic trapping".

We have also applied this stability analysis to other types of focused beams [27] with different NA, and we have found that we can observe complex EFCs whenever the beam has AM.

[1] A. Ashkin, J. M. Dziedzic, J. E. Bjorkholm, and S. Chu, Opt. Lett. **11**, 288 (1986).
[2] D. G. Grier, Nature (London) **424**, 810 (2003).
[3] K. C. Neuman and S. M. Block, Rev. Sci. Instrum. **75**, 2787 (2004).
[4] K. Dholakia *et al.*, Nano Today **1**, 18 (2006); *Advances in Atomic, Molecular, and Optical Physics* (Academic Press, London, 2008), Vol 56, Chap. 6.
[5] L. Allen *et al.*, Phys. Rev. A **45**, 8185 (1992); *Optical Angular Momentum* (IOP Publishing, London, 2003).
[6] A. T. O'Neil and M. J. Padgett, Opt. Commun. **185**, 139 (2000).
[7] H. Rubinsztein-Dunlop *et al.*, Adv. Quantum Chem. **30**, 469 (1998).
[8] V. Garces-Chavez *et al.*, Phys. Rev. A **66**, 063402 (2002).
[9] A. T. O'Neil *et al.*, Phys. Rev. Lett. **88**, 053601 (2002).
[10] M. Funk *et al.*, Opt. Lett. **34**, 139 (2009).
[11] J. Courtial *et al.*, Opt. Commun. **144**, 210 (1997).
[12] S. M. Barnett and L. Allen, Opt. Commun. **110**, 670 (1994).
[13] H. He *et al.*, Phys. Rev. Lett. **75**, 826 (1995).
[14] N. B. Simpson *et al.*, Opt. Lett. **22**, 52 (1997).
[15] A. Rohrbach, Phys. Rev. Lett. **95**, 168102 (2005).
[16] N. B. Viana *et al.*, Appl. Phys. Lett. **88**, 131110 (2006); Phys. Rev. E **75**, 021914 (2007).
[17] K. T. Gahagan and G. A. Swartzlander, J. Opt. Soc. Am. B **15**, 524 (1998); **16**, 533 (1999).
[18] N. B. Simpson *et al.*, J. Mod. Opt. **45**, 1943 (1998).
[19] A. Jesacher *et al.*, Opt. Express **12**, 4129 (2004).
[20] K. Ladavac and D. G. Grier, Opt. Express **12**, 1144 (2004).
[21] D. Cojoc *et al.*, Microelectron. Eng. **78–79**, 125 (2005).
[22] A. Alexandrescu, D. Cojoc, and E. DiFabrizio, Phys. Rev. Lett. **96**, 243001 (2006).
[23] D. S. Bradshaw and D. L. Andrews, Opt. Lett. **30**, 3039 (2005).
[24] See,, e.g., P. Glendinning, *Stability, Instability and Chaos* (Cambridge University Press, Cambridge 1994), Chap. 7.
[25] M. E. J. Friese *et al.*, Appl. Opt. **35**, 7112 (1996).
[26] N. R. Heckenberg *et al.*, in *Mechanical Effects of Optical Vortices*, Optical Vortices (Horizons in World Physics) Vol. 228, edited by M. Vasnetsov, (Nova Science Publishers, New York, 1999), pp 75–105.
[27] See supplementary material at http://link.aps.org/supplemental/10.1103/PhysRevLett.104.103601 for a discussion on (I) linear stability analysis, (II) the eigen force constant for various types of trapping beams, and (III) optical trapping by cylindrically symmetric beams.
[28] L. Novotny and B. Hecht, *Principles of Nano Optics* (Cambridge University Press, New York, 2006).
[29] Y. Zhao *et al.*, Phys. Rev. Lett. **99**, 073901 (2007).
[30] J. Ng *et al.*, Phys. Rev. B **72**, 085130 (2005).
[31] M. I. Antonoyiannakis and J. B. Pendry, Phys. Rev. B **60**, 2363 (1999).
[32] A. A. Neves *et al.*, Opt. Express **14**, 13101 (2006).